Molecular diversity and amino acids evolution in simulated carbonaceous chondrites parent bodies.

A. Garcia[1], Y. Yan[2,3], C. Meinert[4], P. Schmitt-Kopplin[2,3], V. Vinogradoff[1], J-C Viennet[5,6], L. Remusat[5], S. Bernard[5], M. Righezza[1], L. Le Sergeant d'Hendecourt[1], G. Danger[1,7*]

[1] Aix-Marseille Université, CNRS, Institut Origines, Laboratoire PIIM, Marseille, France

[2] Helmholtz Zentrum München, Analytical BioGeoChemistry, Neuherberg, Germany.

[3] Technische Universität München, Chair of Analytical Food Chemistry, Freising-Weihenstephan, Germany.

[4] Université Côte d'Azur, Institut de Chimie de Nice, UMR 7272 CNRS, F-06108 Nice, France

[5] Muséum National d'Histoire Naturelle, Sorbonne Université, UMR CNRS 7590, Institut de minéralogie, de physique des matériaux et de cosmochimie, Paris, France

[6] Université de Lille, CNRS, INRAE, Centrale Lille, UMR 8207-UMET-Unité Matériaux et Transformations, F-59000 Lille, France

[7] Institut Universitaire de France (IUF), France

*gregoire.danger@univ-amu.fr

ABSTRACT:

Organic matter in interplanetary bodies, particularly in parent bodies of carbonaceous chondrites, displays diverse molecules generated in different environments of the Solar nebula. In this study, we simulate the solid phase environment in the laboratory to trace the step-by-step evolution of organic matter from dense molecular cloud ices to processes in meteorite parent bodies. This evolution have shown to lead to an important molecular diversity. Among molecules formed, we focus on amino acids considered as possible chemical tracers of secondary alteration on asteroids. Using gas chromatography and high-resolution mass spectrometry, we detected amino acids in trace amounts in a pre-accretional organic analog formed from dense molecular ice analogs. This analog was then subjected to aqueous alteration at different temperatures and durations. Water induced a complex reactivity leading to increased formation of α- and β-amino acids over time. The initial formation involved reactions between sugars and amine compounds, followed by amino acid destruction, due to the Maillard reaction consuming both sugars and amino acids, hypothesis supported by high resolution mass spectrometry data. Surprisingly, a second phase of amino acid formation, specifically α-amino acids, was observed, indicating the possible occurrence of the Strecker reaction. These findings demonstrate the complex chemical network occurring in presence of a molecular diversity as possibly taking place during parent body alteration. This implies that amino acids detected in various meteorites could have formed through different pathways depending on the initial content of amino acid precursors and on the level and duration of the aqueous alteration.

Keywords: amino acids, GC-FT-Orbitrap-MS, gas chromatography, high-resolution mass spectrometry, ice analogs, meteorite.

1. INTRODUCTION

Studying comets and asteroids can provide insight into the origins of our solar system [1]. These objects are believed to have undergone minimal alterations since their formation [2], making them valuable probes of the early history of the solar system. Space probes such as Rosetta have analyzed the organic content of comets like 67P/Tchourioumov-Guerassimenko and found a high molecular diversity, including both organic and inorganic compounds [3]. The Hayabusa2 mission also discovered a significant molecular diversity on the surface of the Ryugu asteroid [4], with amino acids [5] and nucleobases [6] being identified through targeted analyses. Additionally, carbonaceous chondrites provide information on the organic content of asteroids[7], with up to 5% of their weight being organic matter divided into insoluble and soluble fractions. Both fractions present an important molecular diversity [8,9]. The insoluble fraction may consist of hydrophobic macromolecules interacting with smaller hydrophobic molecules [9], while the soluble fraction presents the highest molecular diversity, containing polyaromatic hydrocarbons, sugars, nucleobases as well as amino acids [10–13]. Some of these amino acids have been detected with slight enantiomeric excesses, which could provide a possible scenario for the emergence of homochirality on Earth. These meteoritic amino acids may also serve as markers of chemical evolution of parent bodies [14,15] as different chemical reactions can lead to their formation depending on their configuration, precursors, and/or environment.

However, meteorites only reveal the final stage of evolution of their parent body history. Laboratory experiments have been developed to obtain a comprehensive understanding of the origin and evolution of organic matter in asteroids and comets. These experiments simulate the evolution of dense molecular cloud ices that occurred during the formation and evolution of the solar nebula. Small molecules like H_2O, NH_3, CH_3OH, CO_2, and CO are deposited onto a cold substrate to form an analog of interstellar ices observed in dense molecular clouds. When these ice analogs are exposed to energetic particles, such as UV photons at Lyman α, ion or electrons bombardment, and subsequently warmed to 300 K to simulate the natural evolution of minor bodies in the solar system, a significant molecular diversity is generated [16]. Targeted analyses of these experiments have detected nucleobases [17,18], sugars [19] and amino acids [20]; suggesting that the protoplanetary disk were already rich in organic molecules before accretion. Comparisons between the amino acid content of such pre-accretional laboratory analog and CM meteorites recovered after the same treatment with acid hydrolysis at 100 °C, a procedure generally used to recover amino acids in meteorites, reveal similarities between that pre-accretional laboratory analogs and the least altered CM chondrites [21]. However, pre-accretional analogs still differ from the organic content of meteorites [22] likely due to the secondary evolution happening in the meteorite parent bodies that influences the molecular inventory.

To simulate this evolution, pre-accretional ice analogs were subjected to aqueous alteration in laboratory experiments. This resulted in the complete transformation of its molecular content [23] while retaining molecular diversity. In this contribution, new experiments are presented on the simulation of the formation and evolution of organic matter from molecular ices in dense clouds to its incorporation inside asteroids, where it may have undergone an aqueous reaction. In this study, the evolution of amino acids was monitored depending on temperature and duration of experiments to obtain information on chemical pathways leading to amino acids in the presence of a high molecular diversity. Analyses were performed using a gas chromatography coupled to high-resolution mass spectrometer (GC-FT-Orbitrap-MS). The amino acids were initially searched for in the pre-accretional analog, and after its incubation at different temperatures (5 °C and 150 °C) for up to 100 days. Different evolution patterns were observed based on the amino acid configurations (α vs. β), suggesting distinct chemical pathways occurring at various times. FT-ICR data from our previous work [23] were also used to strengthen hypotheses of proposed reaction.

2. RESULTS

A pre-accretional analog was formed from a photo-processed ice mixture of $H_2O:CH_3OH:NH_3$ with a ratio of 3:1:1 at Lyman α and 77 K. The experimental procedure leads to the formation of an important molecular diversity as demonstrated by previous work [16,24]. GC-FT-orbitrap-MS was used to identify amino acids following their derivatization [25]. To avoid any analytical bias due to potential contamination of biological L-amino acids, only the D form of chiral amino acids was reported here, utilizing enantioselective separation.

Table 1 – Amino acids identified in the pre-accretional analog before (stored at -30 °C) and after different chemical treatments, (with 6N HCl at 110 °C, in pure H_2O at 5°C or 150°C for 1 or 150 days). id: identified/non-quantified, nd: non-detected.

Amino acids	**configuration**		**Pre-accretional analog**								
			stored dry at -30°C *	**6N HCl 110 °C**		**H_2O 5 °C**		**H_2O 150 °C**			
	#C	**α or β**		**1 day concentration (M)**	**σ (%)**	**100 days concentration (M)**	**σ (%)**	**1 day concentration (M)**	**σ (%)**	**100 days concentration (M)**	**σ (%)**
glycine	2	α	id	5.36×10^{-4}	3.7	7.70×10^{-7}	2.6	3.23×10^{-5}	1.2	1.85×10^{-5}	0.5%
D-alanine	3	α	nd	9.27×10^{-5}	2.3	3.80×10^{-7}	2.0	1.34×10^{-6}	4.6	2.54×10^{-6}	6.5%
β-	3	β	id	1.08×10^{-5}	4.6	id		2.11×10^{-6}	7.2	nd	

alanine										
sarcosine	3	α	id	2.09×10^{-5}	2.3	1.01×10^{-7}	3.7	1.58×10^{-6}	4.5	1.69×10^{-6}	2.8
D-2-ABA	4	α	nd	2.41×10^{-6}	1.7	nd		id		2.01×10^{-7}	5.0
D-3-ABA	4	β	nd	id		nd		id		nd	
D-aspartic acid	4	α	id	id		id		id		nd	
D-valine	5	α	nd	id		nd		nd		id	
D-leucine	6	α	nd	id		id		nd		id	

* The pre-accretional analog was stored at -30 °C under dry condition to limit is potential evolution.

Initially, the presence of only four amino acids (glycine, β-alanine, sarcosine and D-aspartic acid) was detected in the untreated pre-accretional analog (stored in dry conditions at -30 °C). A fraction of this analog sample was incubated in water at 5 °C, resulting in an increase of detected amino acids after 100 days. D-alanine and D-leucine were additionally detected to the initial four amino acids, while the concentration of glycine and β-alanine also increased significantly (estimated at six times for glycine) (Figure 1). This observation indicates that the pre-accretional analog is highly reactive even at low temperature and contains amino acid precursors. After just one day of reaction simulating aqueous alteration at 150 °C, seven amino acids were detected, including glycine, D-alanine, β-alanine, sarcosine, D-2-ABA, D-3-ABA, and D-aspartic acid, but larger α-amino acids, D-valine and D-leucine, were not observed. The concentrations of D-alanine and β-alanine were multiplied by ten, and that of glycine by 100 compared to 100 days at 5 °C (Figure 1). After 100 days at 150 °C, D-valine and D-leucine were observed, but β-amino acids and D-aspartic acid were no longer detected (Table 1). A fraction of the initial pre-accretional analog was also treated with 6N HCl at 110 °C for 24h, which is commonly performed to investigate amino acids in water extracts of meteorites. This treatment led to a significant increase in the number and concentration of detected amino acids compared to the untreated sample (Figure S1). All previously identified amino acids were present, including glycine, D-alanine, β-alanine, sarcosine, D-2-ABA, D-3-ABA, D-aspartic acid, D-valine and D-leucine. Moreover, their concentration increased significantly compared to the non-treated sample (Figure S1). This proves that the pre-accretional analog, as well as water extracts of meteorite, contain amino acid precursors that can easily undergo hydrolysis.

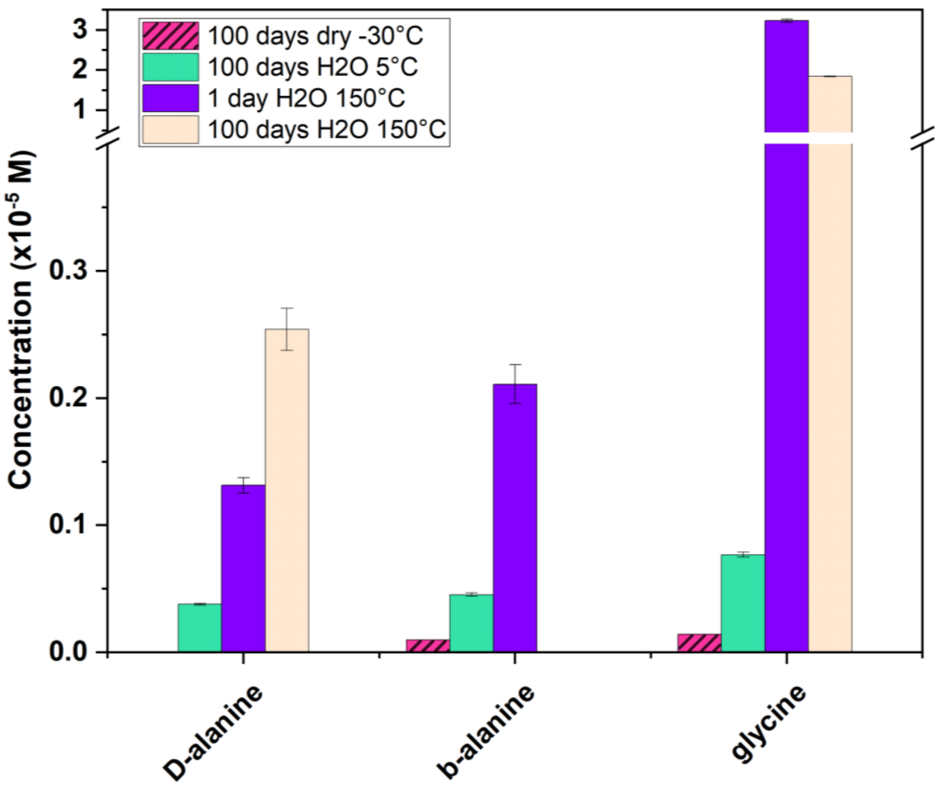

Figure 1 – Concentration of D-alanine, β-alanine and glycine for the initial pre-accretional analog (stored at -30 °C under dry condition), and after 100 days in water at 5 °C or 150 °C. β-Alanine and glycine in the

pre-accretional analog (dry at -30 °C) are dashed because their detected peak areas are below the quantification limit.

The evolution of the time profile of the amino acids presented in Table 1 was monitored at a temperature of 150 °C. The only amino acids that could be quantified were glycine, D-alanine, sarcosine and β-alanine. For the remaining amino acids, only a qualitative profile based on absolute intensities is discussed. Figure 2 and S2 depict the overall evolution of amino acids (in concentration or absolute intensities), revealing three distinct evolution profiles. A rapid increase in amino acid abundances occurs during the first 3 days of incubation, with the exception of D-valine and D-leucine, which were not identified. After one day for glycine and 3 days for other amino acids, there was a significant decrease in their abundance. Notably, after 10 days of incubation, the evolution of amino acids varied depending on their configuration. The β-amino acids, such as β-alanine and D-3-ABA, tend to disappear completely, while α-amino acids present a new increase in their abundances, including the notable emergence of D-valine and D-leucine. Only α-aspartic acid showed a similar profile to β-amino acids. After 30 days of incubation, D-valine and D-leucine tend to decrease, while other α-amino acids continue to increase. These distinct evolution patterns suggest the occurrence of various chemical pathways.

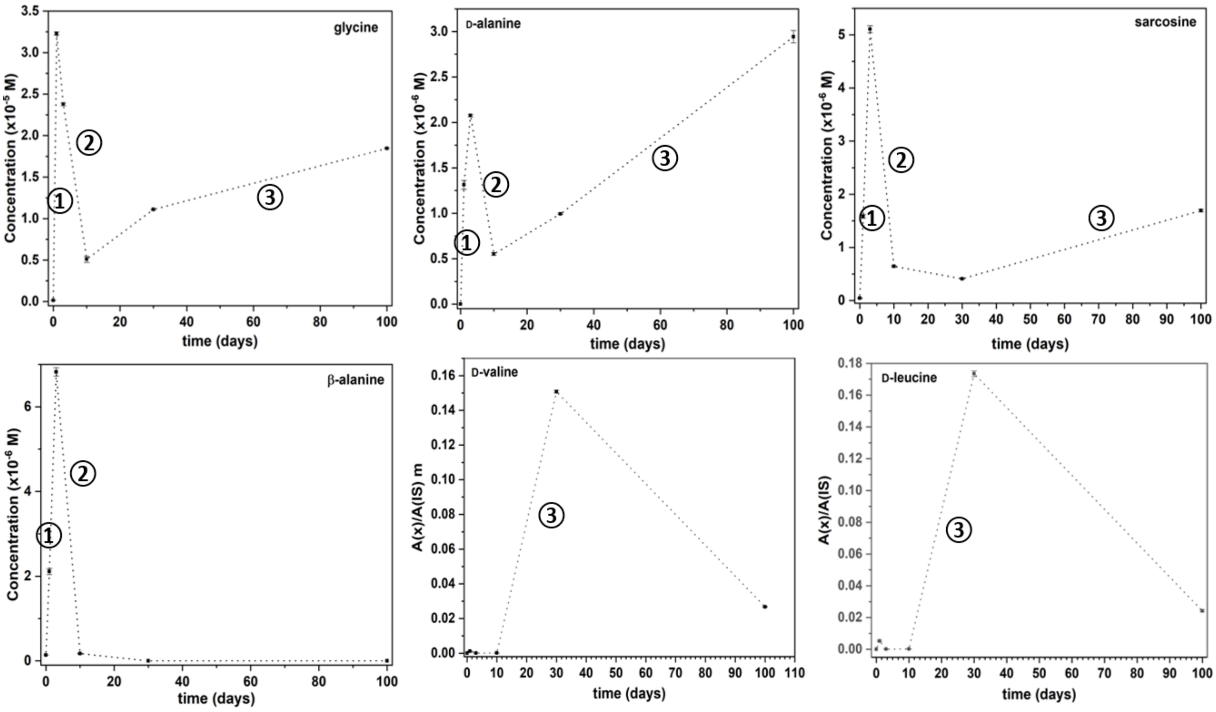

Figure 2 –Monitoring of several amino acids in a pre-accretional analog incubated in water at 150 °C. The different phases of amino acid evolution are also indicated as ①, ② and ③. More details on these different phases are discussed in the main text. For glycine, alanine, sarcosine and β-alanine, quantifications are performed by following the procedure published in Garcia *et al.* 2023. For valine and leucine with abundances lower than their LOQ, only the qualitative evolution $A_{(x)}/A_{(IS)}$ of their relative integrated area ($A_{(x)}$) to the one of internal standard ($A_{(IS)}$) are displayed. The dotted lines are reported solely as a visual guide.

3. DISCUSSION

The organic material of the pre-accretional analog is highly reactive and efficiently evolves in the presence of water, as demonstrated by the experiment in H_2O conducted at 5 °C and 150°C. There is a significant chemical evolution at the molecular level. The high molecular diversity of the analog [16] results in various chemical reactions, affecting amino acid formation.

The initial analog (stored under dry condition at -30 °C) exhibits a low diversity and abundance of amino acids. Glycine, β-alanine, sarcosine and aspartic acid are only detected as trace amounts below their limit of quantification. These amino acids are directly related to the photo-processing of the initial ice and its subsequent warming to room temperature. The formation of glycine in ice analog can occur following different pathways. It may occur through ice processing via the transformation of methyl carbamate into glycinate salt under UV irradiation (Figure 3A) [26,27], as supported by the detection of methylamine in pre-accretional analogs [28]. No investigation has been conducted on the formation of the other three amino acids, making it difficult to propose hypotheses about their formation mechanism in such ices. The Strecker synthesis has been shown to occur partially during photo-processing and heating of ices, since its last step, which consists in the hydrolysis of the amino nitrile, is not possible in these conditions due to a high energy barrier [29–31], which prevents the formation of glycine. Nonetheless, radical and thermal chemistries is likely to play an important role in their formation (Figure 3B) [32,33].

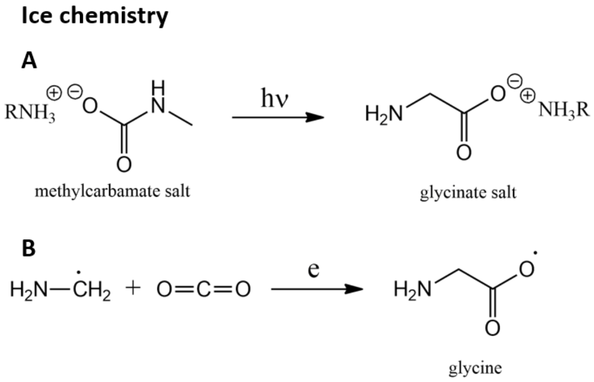

Figure 3 – Potential chemical reactions occurring during the initial processing of interstellar ice analogs and leading to the formation of glycine formation. The reaction occurs at low temperature (77 K) and pressure (10^{-8} mbar) under UV irradiation at 121 nm.

After incubating the analog in water at 150 °C, a rapid increase in amino acid abundances was observed, except for D-valine and D-leucine, which appear only after 30 days. If the Strecker synthesis would be involved in amino acid formation, the absence of valine and leucine within the first 30 days suggests that this process alone cannot explain the formation of α-amino acids. In addition to glycine, D-alanine, sarcosine, D-aspartic acid and β-alanine are also formed, which may be the result of the reaction of carbohydrates present in the analog [19,34–37] with ammonia or methylamine (Figure 4). This scenario is strengthened by kinetic profiles that show the involvement of carbohydrates in amino acid formation from a formaldehyde mixture at high temperatures [38]. A rapid increase of amino acid formation is also observed followed by a rapid decrease of amino acid abundance in the same time range as observed in our experiment. In this scenario, glycine and sarcosine can be formed from glycolaldehyde (Figure 4A) [39], whereas β-alanine could arise from the reaction between glyceraldehyde and ammonia. D-alanine can be produced by isomerization of dihydroxyacetone, which reacts with ammonia (Figure 4B). Aspartic acid can be formed by the reaction of ammonia with erythrulose (Figure 4C). D-2-ABA and D-3-ABA can be generated also from sugars or sugar acids [38].

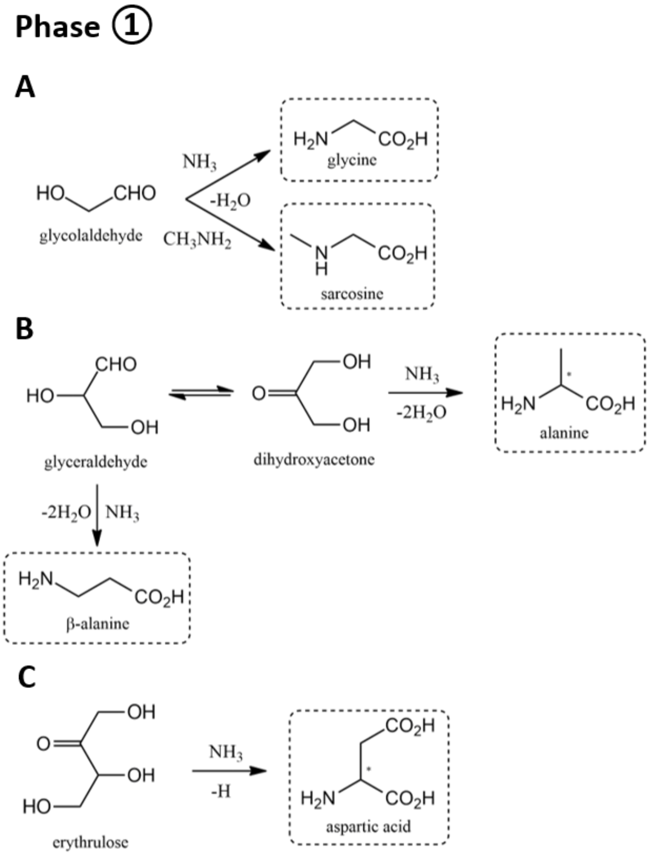

Figure 4 – Potential chemical reactions leading to α- and β-amino acids during the early stages of incubating a pre-accretional analog in water at 150 °C.

Following a 3-day incubation period (phase 2, Figure 2), there is a strong reduction in the abundance of amino acids, suggesting that the previous reservoir (phase 1, Figure 2) of amino acid precursors has been either consumed or destroyed. A such strong decrease cannot be explained only by amino acid degradation leading to CO_2 and NH_3 release [38,40]. Reactions between amino acids and other compounds like urea [41] can occur, leading to the formation of carbamoyl amino acids that give back amino acids [42,43]. However, to explain this profile, a simultaneous consumption of amino acid precursors and amino acids may be required. A potential explanation would be the Maillard reaction (Figure 5), where amino acids react with sugars leading to the consumption of both amino acids and sugars [44].

To verify this hypothesis, stoichiometric formula of products resulting from the Maillard reaction (Amadori product (ARP), Figure 5) where searched in high-resolution mass spectrometry data of the same samples (data published in Danger et al. [23]). Table S1 shows the possible ARPs and their sum formulas based on the expected reaction between the experimentally found amino acids (alanine/sarcosine, glycine, aspartic acid, valine, leucine, 2-ABA, 3-ABA) and reducing sugars with basic CH_2O unit from 2 to 6. All potential formulas were found in the experimental data during all the hydrothermal process. ARPs are already present in non-negligible amounts in the original pre-accretional analog that was conserved at -30°C (Figure S5). Keeping the original sample in water at cold temperature (5°C) changed slightly the concentration of the ARPs, some being degraded, others being produced. The kinetic from 1 day to 100 days at 150°C showed a combined effect of (i) disappearance of the ARPs, further engaged in reactions and (ii) further reactivity of the amino acids with reducing sugars in heated solution, following Maillard reactions and leading to the same ARP. At the beginning of the reaction, the hydrothermal process generated more ARPs, due to the reaction of the amino acids with the present reducing sugars (Figure S6). Interestingly, the profiles of the ARPs follow the profiles of the amino acid concentration in the first 30 days of the process in similar phases 1, 2, 3 and confirm the differential kinetics in the formation of novel amino acids via the Strecker reaction and their relative consumption and successive formation of ARPs via the Maillard hydrothermal reaction. After 30 days of processing, the formation of ARPs decreased due to the limited availability of precursor-reducing sugar. As the degradation of ARPs continued, their intensity kept decreasing. It has to be noted, that while with GC-FT-OrbitrapMS analyses, valine is not detected, FT-ICR-MS analyses suggest the formation of its ARP product at low duration, which is not the case for leucine. It seems that valine is also present in the initial pre-accretional analog.

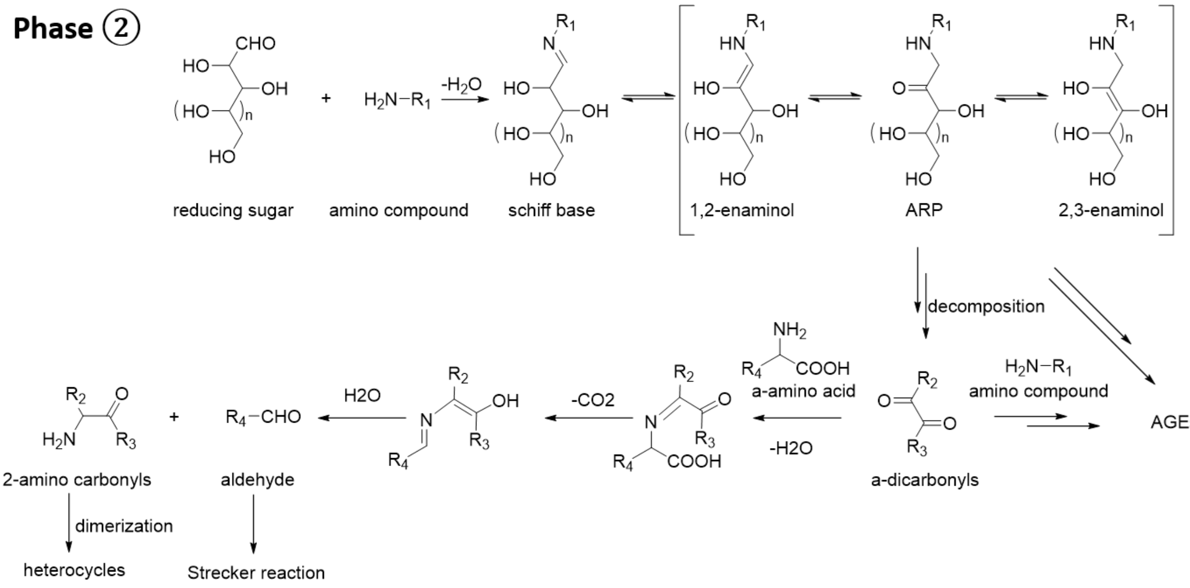

Figure 5 – Maillard reaction may lead to amino compound degradation during Phase 2 with incubation of a pre-accretional analog in water at 150 °C. Reducing sugar can react with the amine group of amino compounds to form a Schiff base, followed by the Amadori rearrangement to an Amadori product (ARP). Decomposition of ARP by fragmentation of the carbohydrate backbone can generate various α-dicarbonyls. Only α-amino acids can undergo α-dicarbonyls-assisted oxidative decarboxylation and form aldehydes, which could form some α-amino acids at Phase 3 by Strecker reaction. α-dicarbonyls can also react with amino compounds to produce stable advanced glycation end products (AGEs).

After ten days of incubation, a new evolution of amino acid formation occurs. This phase 3 is characterized by the formation of only α-amino acids, including glycine, D-alanine, D-2-ABA, sarcosine, D-valine and D-leucine, while D-aspartic acid disappears completely, along with β-amino acids (β-alanine and D-3-ABA). This implies a chemical reaction specific to the formation of aliphatic α-amino acids, such as the Strecker synthesis (Figure 6), which is known to produce α-amino acids during aqueous alteration in meteorite's parent bodies [45,5]. During the first days of incubation, the aqueous alteration causes a transformation of the initial molecules of the pre-accretional analog [23], leading to the formation of aldehydes, NH_3 and HCN into the aqueous environment. As previously noted, some aldehydes may be formed from Strecker degradation or Amadori rearrangement products [46,47] of the Maillard reaction occurring in Phase 2 (Figure 5). Aspartic acid is not formed after ten days, which indicates that its aldehyde precursor is not available or that aspartic acid is present at a concentration below our detection limit. Different intensity profiles are observed for α-amino acids, with D-valine and D-leucine showing a decrease in abundances after 30 days of reaction, while other α-amino acids continue to rise. This could be due to the limited availability of aldehyde precursors for valine and leucine compared to formaldehyde and acetaldehyde for glycine and alanine, respectively. Generally, the formation of aldehydes and their precursors from the initial ice photo-processing involves free-radical chemistry, which leads to a decrease in compound abundance with an increase in carbon number and ramification [48]. Therefore, the initial abundance of more complex aldehydes and their corresponding amino acids is expected to be lower than that of simpler α-amino acids.

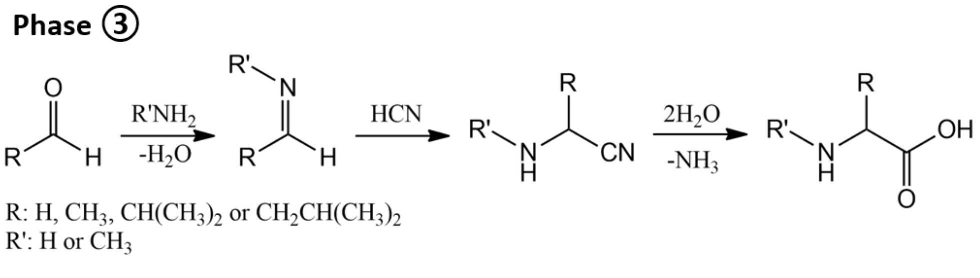

Figure 6 – Strecker reaction likely occurring during phase 3, resulting in the formation of only α-amino acids.

A fraction of the precursors of organic matter found in carbonaceous chondrites is believed to originate from dense molecular cloud ices [49–51]. This scenario is strengthened by analyses of samples returned from the Ryugu asteroid [4]. However, the present experiments demonstrate that these ices can only generate a limited diversity and quantity of amino acids due to insufficient available energy. Investigations into the Strecker synthesis of α-amino acids from these ices has demonstrated this limitation [31,52–54]. Therefore, by considering only ices, the total amount of amino acids incorporated inside parent bodies of carbonaceous chondrites is expected to be low. Nonetheless, one must emphasize that the high molecular diversity generated during the ice processing present numerous amino acid precursors [19,48,55], next to others sources of amino acids possibly present in the disk.

This pre-accretional organic matter is highly reactive and is susceptible to undergo a secondary evolution inside meteorite parent bodies, as shown by laboratory experiments [56]. Meteorite analyses have indeed demonstrated that aqueous alteration has occurred within their parent bodies [57–60], a fact confirmed by the analyses of samples returned from the Ryugu asteroid [4,61]. As shown in this work, when a pre-accretional organic analog is placed in water according to this alteration scenario, its molecular diversity evolve [23] and leads to the formation of numerous amino acids, with increasing formation rates as the temperature increases. Furthermore, depending on the time of aqueous alteration, different chemical pathways occur leading to variation in abundances and types of amino acids. Other targeted analyses on amino acids on similar analogs altered at 125 °C showed also weak evolution of several amino acids [28]. The concentration of α-amino acids (glycine, alanine and serine) tends to increase with time, while the concentration of β-alanine decreases. Trends observed in Qasim et al. are less pronounced than in our experiment, probably because of the differences of experimental conditions compared to our conditions, since they use lower temperatures (125 °C vs. 150 °C) and lower duration experiments (30 days vs. 100 days). In this evolution, sugars play an important role in amino acid formation at short durations or low temperatures, as shown here, whereas the Strecker synthesis plays this role at longer durations. Since amino acid precursors differ between these two reactions, the amino acids finally formed differ in content and amount. At short reaction times, small α-amino acids (glycine, alanine, sarcosine, 2-ABA) are formed, along with β-amino acids (β-alanine, 3-ABA). At longer durations, β-amino acids disappear entirely, and more complex α-amino acids are formed. Further experiments are needed to monitor the evolution of sugars in order to compare it with the evolution of amino acids to definitively validate this scheme. The present experiment indicates that the complexity of amino acids observed in carbonaceous meteorites and asteroids probably originated from secondary processing, and not directly from the ice chemistry, and depends on the molecular diversity generated from the initial ice. The formation of amino acids in such object is thus related to a complex chemical network has observed in our present experimental work.

However, the laboratory study of the evolution of the pre-accretional analog in an aqueous environment suggests that a higher presence of β-amino acids should indicate a lower aqueous alteration, while a higher presence of α-amino acids on longer alteration period. For instance, higher β-alanine/glycine are observed at lower degree of alteration of pre-accretional analogs (Table 1). This finding is corroborated by similar aqueous alteration experiments performed by Qasim *et al.* [28] on a similar pre-accretional material. At the contrary, in meteorites, it is proposed that lower degree of aqueous alteration favors the presence of α-amino acids via the Strecker synthesis, while higher degree of alteration enhances the presence of β-amino acids compared to α-amino acids [21,62,63]. Therefore, higher β-alanine/glycine ratios are observed for more aqueous altered meteorite. These discrepancies could be due to factors as the influence of minerals (absent in our experiments), different alteration timeframes, or additional origins of amino acids or their precursors. Further experiments have to explore these hypotheses.

4. MATERIAL AND METHODS

4.1 Chemicals and solutions

For amino acid analyses, each amino acid standard was prepared individually and then mixed together in 0.1 M hydrochloric acid (HCl) to obtain a stock solution of 10^{-4} M. Serial dilutions were prepared for calibration curves. The 0.1 M HCl solution was prepared by diluting 6N HCl (specific ampoule for amino acid analysis, Merck) in ultra-pure water produced by a Direct-Q® 3 UV water purification system. All amino acids and chemicals used were from Sigma-Aldrich, Fluka, or Acros Organics. For more information see Garcia et al. 2023 [25].

4.2 Derivatization procedure

Amino acid solutions were derivatized into their *N* (*O*, *S*)-ethoxy-carbonylheptafluorobutylester (ECHFBE) derivatives according to the protocol developed by Meinert et *al.* [64]. In a conical reaction flask (Reactivial, Thermo Scientific™), a 10 µL volume of aqueous amino acid solution in 0.1 M HCl reacted with 3.8 µL of 2,2,3,3,4,4,4-heptafluoro-1-butanol and 1.2 µL of pyridine. After 15 s of stirring, 1 µL of ethyl chloroformate were added and the resulting solution stirred vigorously for 15 seconds. The ECHFBE derivatives were extracted with 10 µL of a 10^{-5} M methyl laurate (internal standard) chloroform solution. The organic phase containing the ECHFBE derivatives was then transferred into 1 mL GC vials equipped with 100 µL inserts for GC-FT-Orbitrap-MS analysis. Note that this derivatization method does not provide identical yields among different amino acid groups, especially discriminating α, α-dialkyl amino acids as well as γ-amino acids [25,65]. Each sample was injected in triplicate to obtain information on the instrument repeatability.

4.3 Post-analysis data processing

All data were acquired in TIC and processed with Qual Browser Xcalibur. For each amino acid, the search and identification was performed by mass extraction, based on the retention time and a specific mass/charge ratio *(m/z)* for each amino acid (amino acid databases [25]). The monitoring of amino acid profiles was performed by integrating the characteristic ion of each amino acid A(x) divided by the integrated area of the internal standard A(IS), A(x)/A(IS). To correct for possible contamination, the values obtained were subtracted from a derivatization blank, which consists in 0.1 M HCl solvent used for the dilution of the amino acids, to which the derivatization step was applied. Corrected data result in $A(x)/A(IS)-A(x)_b/A(IS)_b$. Only concentrations of amino acids that are equal or above the quantification limit are indicated [25], while amino acids whose values are between detection and quantification limits are only indicated as identified.

4.4 Synthesis of pre-accretional organic analogs to post-accretional organic material

A pre-accretional organic analog was formed from an ice including H_2O, $^{12}CH_3OH$ and NH_3 in proportion of 3:1:1. The corresponding gas mixture was deposited in a stainless steel chamber on a copper cold finger at low pressure (10^{-7} to 10^{-8} mbar) and low temperature (77 K) forming an ice, analog to the ones observed in dense molecular clouds on silicate grains[66]. The ice formation was concomitant to its irradiation with a dihydrogen UV microwave discharge lamp (mainly emitting at 121 nm) to simulate stellar radiation. After 72 h of deposition and simultaneous irradiation, the photo-processed ice was slowly heated to 300 K to obtain an analog of pre-accretional organic matter. Aqueous alteration experiments were conducted with 100 µL of the pre-accretional analog dissolved in milli-Q water at a concentration of 1 g L^{-1} (more details in Danger et al. 2021 [23]). Sealed gold capsules were hold at 5 °C (100 days) or 150 °C for varying length of time (1, 3, 10, 30 and 100 days). The pressure inside the reactors was not monitored and should correspond to the vapor pressure of water, i.e. up to 5 bars at 150 °C. At the end of the experiments, 10 µL of the 100 µL solution was used for amino acid analyses following the procedure described in section 2.2. Furthermore, one fraction of the initial pre-accretional analogue solution was dried and stored at -30 °C and directly converted into ECHFBE derivatives forming the non-altered sample. Another fraction was recovered in 6N HCl to be hydrolyzed during 24 h at 110 °C followed by the ECHFBE derivatization.

4.5 GC-FT-Orbitrap-MS configuration

Analyses were performed on a Trace 1310 gas chromatograph (GC) coupled to a Q-Exactive Orbitrap™ mass spectrometer (MS) from Thermo Fisher Scientific operated at PIIM. Injections were performed with an auto-sampler (AI 1310 from Thermo Fisher) in splitless mode (splitless time: 1 min) with an injector temperature of 230 °C. Helium was used as carrier gas with a flow rate of 1 mL min^{-1} and a purge rate of 5.0 mL min^{-1}. Amino acids were separated on two Chirasil-L-Val columns (each 25 m x 0.25 mm x 0.12 µm film thickness, Agilent) connected with a Valco connector. The duration of the oven temperature program was 90 min with a solvent delay of 14 min. The optimized temperature program was as follows: 40 °C for 1 min, then increased to 80 °C with a slope of 10 °C min^{-1} during 10 min then 2 °C min^{-1} to reach 190 °C with an isotherm during 20 min. The transfer line was set at 250 °C. The *m/z* range was 50−400 with a FWHM resolution fixed at 60 000, a target AGC value at 10^6 and a max IT at 200 ms. Electron impact ionization was used at 70 eV.

Acknowledgement

The research was funded by the Centre National d'Etudes Spatiales (CNES, R-S18/SU-0003-072 and R-S18/SU-0003-072, PI: G. D.), and the Centre National de la Recherche Française (CNRS) with the programs "Physique et Chimie du Milieu Interstellaire" (PCMI-PI:G.D.) and "Programme National de Planétologie" (PNP) (PI: G.D.). G.D is grateful to the Agence Nationale de la Recherche for funding via the ANR RAHIIA_SSOM (ANR-16-CE29-0015) and VAHIIA (ANR-12-JS08-0001). The project has further received funding from the EXCellence Initiative of Aix-Marseille Université - A*Midex, a French "Investissements d'Avenir programme" AMX-21-IET-018, from the Région SUD Provence Alpes Côte d'Azur "Apog 2017" – PILSE, as well by the EU Framework Program for Research and Innovation Horizon 2020 (grants ERC 804144, ALIFE). L.R. thanks the European Research Council for funding via the ERC project HYDROMA (grant agreement No. 819587).

Reference

1. Caselli, P. & Ceccarelli, C. Our astrochemical heritage. *Astron. Astrophys. Rev.* **20**, 56 (2012).
2. Pizzarello, S., Yarnes, C. T. & Cooper, G. The Aguas Zarcas (CM2) meteorite: New insights into early solar system organic chemistry. *Meteorit. Planet. Sci.* **14**, maps.13532 (2020).
3. Beth, A. *et al.* ROSINA ion zoo at Comet 67P. *Astron. Astrophys.* 1–26 (2020) doi:10.1051/0004-6361/201936775.
4. Naraoka, H. *et al.* Soluble organic molecules in samples of the carbonaceous asteroid (162173) Ryugu. *Science (80-.).* **379**, (2023).
5. Sakaguchi, C. *et al.* Insights into the formation and evolution of extraterrestrial amino acids from the asteroid Ryugu. *Nat. Commun.* **14**, 1482 (2023).
6. Oba, Y. *et al.* Uracil in the carbonaceous asteroid (162173) Ryugu. *Nat. Commun.* **14**, 1292 (2023).
7. Abreu, N. M., Aponte, J. C., Cloutis, E. A. & Nguyen, A. N. The Renazzo-like carbonaceous chondrites as resources to understand the origin, evolution, and exploration of the solar system. *Geochemistry* **80**, 125631 (2020).
8. Schmitt-Kopplin, P. *et al.* High molecular diversity of extraterrestrial organic matter in Murchison meteorite revealed 40 years after its fall. *Proc. Natl. Acad. Sci. U. S. A.* **107**, 2763–2768 (2010).
9. Danger, G. *et al.* Unprecedented Molecular Diversity Revealed in Meteoritic Insoluble Organic Matter: The Paris Meteorite's Case. *Planet. Sci. J.* **1**, 55 (2020).
10. Pizzarello, S.; Cooper, G. W.; Flynn, G. J. The Nature and Distribution of the Organic Material in Carbonaceous Chondrites and Interplanetary Dust Particles. in *Meteorites and the Early Solar System II* p.625-651 (2006).
11. Callahan, M. P. *et al.* Carbonaceous meteorites contain a wide range of extraterrestrial nucleobases. *Proc. Natl. Acad. Sci. U. S. A.* **108**, 13995–13998 (2011).
12. Furukawa, Y. *et al.* Extraterrestrial ribose and other sugars in primitive meteorites. *Proc. Natl. Acad. Sci.* **116**, 24440–24445 (2019).
13. Lecasble, M., Remusat, L., Viennet, J.-C., Laurent, B. & Bernard, S. Polycyclic aromatic hydrocarbons in carbonaceous chondrites can be used as tracers of both pre-accretion and secondary processes. *Geochim. Cosmochim. Acta* **335**, 243–255 (2022).
14. Elsila, J. E. *et al.* Meteoritic Amino Acids: Diversity in Compositions Reflects Parent Body Histories. *ACS Cent. Sci.* acscentsci.6b00074 (2016) doi:10.1021/acscentsci.6b00074.
15. Burton, A. S., Stern, J. C., Elsila, J. E., Glavin, D. P. & Dworkin, J. P. Understanding prebiotic chemistry through the analysis of extraterrestrial amino acids and nucleobases in meteorites. *Chem. Soc. Rev.* **41**, 5459–72 (2012).
16. Danger, G. *et al.* Characterization of laboratory analogs of interstellar/cometary organic residues using very high resolution mass spectrometry. *Geochim. Cosmochim. Acta* **118**, 184–201 (2013).

17. Ruf, A. *et al.* The Challenging Detection of Nucleobases from Pre-accretional Astrophysical Ice Analogs. *Astrophys. J. Lett.* **887**, L31 (2019).

18. Oba, Y., Takano, Y., Naraoka, H., Watanabe, N. & Kouchi, A. Nucleobase synthesis in interstellar ices. *Nat. Commun.* **10**, 4413 (2019).

19. Meinert, C. *et al.* Ribose and related sugars from ultraviolet irradiation of interstellar ice analogs. *Science (80-.).* **352**, 208–212 (2016).

20. Muñoz Caro, G. M. *et al.* Amino acids from ultraviolet irradiation of interstellar ice analogues. *Nature* **416**, 403–406 (2002).

21. Modica, P., Martins, Z., Meinert, C., Zanda, B. & d'Hendecourt, L. L. S. The Amino Acid Distribution in Laboratory Analogs of Extraterrestrial Organic Matter: A Comparison to CM Chondrites. *Astrophys. J.* **865**, 41 (2018).

22. Danger, G. *et al.* The transition from soluble to insoluble organic matter in interstellar ice analogs and meteorites. *Astron. Astrophys.* (2022) doi:10.1051/0004-6361/202244191.

23. Danger, G. *et al.* Exploring the link between molecular cloud ices and chondritic organic matter in laboratory. *Nat. Commun.* **12**, 1–9 (2021).

24. Danger, G. *et al.* Insight into the molecular composition of laboratory organic residues produced from interstellar/pre-cometary ice analogues using very high resolution mass spectrometry. *Geochim. Cosmochim. Acta* **189**, 184–196 (2016).

25. Garcia, A. *et al.* Gas chromatography coupled-to Fourier transform orbitrap mass spectrometer for enantioselective amino acid analyses: Application to pre-cometary organic analog. *J. Chromatogr. A* **1704**, 464118 (2023).

26. Bossa, J. B. *et al.* Methylammonium methylcarbamate thermal formation in interstellar ice analogs: a glycine salt precursor in protostellar environments. *Astron. Astrophys.* **506**, 601–608 (2009).

27. Bossa, J. B., Borget, F., Duvernay, F., Theulé, P. & Chiavassa, T. How a usual carbamate can become an unusual intermediate: a new chemical pathway to form glycinate in the interstellar medium. *J. Phys. Org. Chem.* **23**, 333–339 (2010).

28. Qasim, D. *et al.* Meteorite Parent Body Aqueous Alteration Simulations of Interstellar Residue Analogs. *ACS Earth Sp. Chem.* (2023) doi:10.1021/acsearthspacechem.2c00274.

29. Singh, S. K., Zhu, C., La Jeunesse, J., Fortenberry, R. C. & Kaiser, R. I. Experimental identification of aminomethanol (NH2CH2OH)—the key intermediate in the Strecker Synthesis. *Nat. Commun.* **13**, 375 (2022).

30. Danger, G. *et al.* Experimental investigation of aminoacetonitrile formation through the Strecker synthesis in astrophysical-like conditions: Reactivity of methanimine (CH<inf>2</inf>NH), ammonia (NH<inf>3</inf>), and hydrogen cyanide (HCN). *Astron. Astrophys.* **535**, (2011).

31. Danger, G., Duvernay, F., Theule, P., Borget, F. & Chiavassa, T. Hydroxyacetonitrile (HOCH2CN) Formation In Astrophysical Conditions. Competition With The Aminomethanol, A Glycine Precursor. *Astrophys. J.* **756**, 11 (2012).

32. Holtom, P. D., Bennett, C. J., Osamura, Y., Mason, N. J. & Kaiser, R. I. A combined experimental and theoretical study on the formation of the amino acid glycine (NH2CH2COOH) and its isomer (CH3NHCOOH) in extraterrestrial ices . *Astrophys. J.* **626**, 940–952 (2005).

33. Theule, P. *et al.* Thermal reactions in interstellar ice: a step towards molecular complexity in the interstellar medium. *Adv. Sp. Res.* **52**, 1567–1579 (2013).

34. Layssac, Y., Gutiérrez-Quintanilla, A., Chiavassa, T. & Duvernay, F. Detection of glyceraldehyde and glycerol in VUV processed interstellar ice analogues containing formaldehyde: a general formation route for sugars and polyols. *Mon. Not. R. Astron. Soc.* **496**, 5292–5307 (2020).

35. Kebukawa, Y., Chan, Q. H. S., Tachibana, S., Kobayashi, K. & Zolensky, M. E. One-pot synthesis of amino acid precursors with insoluble organic matter in planetesimals with aqueous activity. *Sci. Adv.* **3**, e1602093 (2017).

36. Vinogradoff, V. *et al.* Impact of Phyllosilicates on Amino Acid Formation under Asteroidal Conditions. *ACS Earth Sp. Chem.* **4**, 1398–1407 (2020).

37. Koga, T. & Naraoka, H. Synthesis of Amino Acids from Aldehydes and Ammonia: Implications for Organic Reactions in Carbonaceous Chondrite Parent Bodies. *ACS Earth Sp. Chem.* **6**, 1311–1320 (2022).

38. Aubrey, A. D., Cleaves, H. J. & Bada, J. L. The Role of Submarine Hydrothermal Systems in the Synthesis of Amino Acids. *Orig. Life Evol. Biosph.* **39**, 91–108 (2009).

39. YANAGAWA, H., Kobayashi, Y. & Egami, F. Genesis of Amino Acids in the Primeval Sea. *J.Biochem* **87**, 359–362 (1980).

40. Körner, P. Hydrothermal Degradation of Amino Acids. *ChemSusChem* **14**, 4947–4957 (2021).

41. Nuevo, M. *et al.* Urea, glycolic acid, and glycerol in an organic residue produced by ultraviolet irradiation of interstellar/pre-cometary ice analogs. *...Astrobiology* **10**, 245–256 (2010).

42. Danger, G., Boiteau, L., Cottet, H. & Pascal, R. The peptide formation mediated by cyanate revisited. N-carboxyanhydrides as accessible intermediates in the decomposition of N-carbamoylamino acids. *J. Am. Chem. Soc.* **128**, 7412–7413 (2006).

43. Danger, G., Plasson, R. & Pascal, R. Pathways for the formation and evolution of peptides in prebiotic environments. *Chem. Soc. Rev.* **41**, 5416–5429 (2012).

44. Hemmler, D. *et al.* Evolution of Complex Maillard Chemical Reactions, Resolved in Time. *Sci. Rep.* **7**, 3–8 (2017).

45. Elsila, J. E., Dworkin, J. P., Bernstein, M. P., Martin, M. P. & Sandford, S. A. Mechanisms of amino acid formation in interstellar ice analogs . *Astrophys. J.* **660**, 911–918 (2007).

46. YAYLAYAN, V. A. Recent Advances in the Chemistry of Strecker Degradation and Amadori Rearrangement: Implications to Aroma and Color Formation. *Food Sci. Technol. Res.* **9**, 1–6 (2003).

47. Davidek, T., Clety, N., Aubin, S. & Blank, I. Degradation of the Amadori Compound N -(1-Deoxy- d -fructos-1-yl)glycine in Aqueous Model Systems. *J. Agric. Food Chem.* **50**, 5472–5479 (2002).

48. Abou Mrad, N., Duvernay, F., Chiavassa, T. & Danger, G. Methanol ice VUV photo-processing: GC-MS analysis of volatile organic compounds. *Mon. Not. R. Astron. Soc.* **458**, 1234–1241 (2016).

49. Le Guillou, C., Bernard, S., Brearley, A. J. & Remusat, L. Evolution of organic matter in Orgueil, Murchison and Renazzo during parent body aqueous alteration: In situ investigations. *Geochim. Cosmochim. Acta* **131**, 368–392 (2014).

50. Le Guillou, C. & Brearley, A. Relationships between organics, water and early stages of aqueous alteration in the pristine CR3.0 chondrite MET 00426. *Geochim. Cosmochim. Acta* **131**, 344–367 (2014).

51. Vinogradoff, V. *et al.* Paris vs. Murchison: Impact of hydrothermal alteration on organic matter in CM chondrites. *Geochim. Cosmochim. Acta* **212**, 234–252 (2017).

52. Fresneau, A. *et al.* Thermal formation of hydroxynitriles , precursors of hydroxyacids in astrophysical ice analogs : Acetone ((CH 3) 2 C = O) and hydrogen cyanide (HCN) reactivity. *Mol. Astrophys.* **1**, 1–12 (2015).

53. Danger, G. *et al.* Experimental investigation of aminoacetonitrile formation through the Strecker synthesis in astrophysical-like conditions: reactivity of methanimine (CH2NH), ammonia (NH3), and hydrogen cyanide (HCN). *Astron. Astrophys.* **535**, A47 (2011).

54. Fresneau, A. *et al.* Ice chemistry of acetaldehyde reveals competitive reactions in the first step of the Strecker synthesis of alanine : formation of HO – CH (CH 3)– NH 2 vs . HO – CH (CH 3)– CN. *Mon. Not. R. Astron. Soc.* **1660**, 1649–1660 (2015).

55. Vinogradoff, V. *et al.* New insight into the formation of hexamethylenetetramine (HMT) in interstellar and cometary ice analogs. *Astron. Astrophys.* **530**, A128 (2011).

56. Danger, G. *et al.* Exploring the link between molecular cloud ices and chondritic organic matter in

laboratory. *Nat. Commun.* **12**, 3538 (2021).

57. Glavin, D. P. *et al. The Origin and Evolution of Organic Matter in Carbonaceous Chondrites and Links to Their Parent Bodies*. *Primitive Meteorites and Asteroids* (Elsevier Inc., 2018). doi:10.1016/B978-0-12-813325-5.00003-3.

58. Suttle, M. D. *et al.* Alteration conditions on the CM and CV parent bodies – Insights from hydrothermal experiments with the CO chondrite Kainsaz. *Geochim. Cosmochim. Acta* **318**, 83–111 (2022).

59. Jilly-Rehak, C. E., Huss, G. R., Nagashima, K. & Schrader, D. L. Low-Temperature Aqueous Alteration on the Cr Chondrite Parent Body: Implications From in Situ Oxygen-Isotope Analyses. *Geochim. Cosmochim. Acta* **222**, 230–252 (2017).

60. Brearley, A. J. The Action of Water. *Meteorites Early Sol. Syst. II* **943**, 587–624 (2006).

61. Nakamura, T. *et al.* Formation and evolution of carbonaceous asteroid Ryugu: Direct evidence from returned samples. *Science (80-.).* **379**, (2023).

62. Martins, Z., Modica, P., Zanda, B. & d'Hendecourt, L. L. S. The amino acid and hydrocarbon contents of the paris meteorite: Insights into the most primitive cm chondrite. *Meteorit. Planet. Sci.* **50**, 926–943 (2015).

63. Burton, A. S., Grunsfeld, S., Elsila, J. E., Glavin, D. P. & Dworkin, J. P. The effects of parent-body hydrothermal heating on amino acid abundances in CI-like chondrites. *Polar Sci.* **8**, 255–263 (2014).

64. Meinert, C. & Meierhenrich, U. J. Derivatization and Multidimensional Gas-Chromatographic Resolution of α-Alkyl and α-Dialkyl Amino Acid Enantiomers. *Chempluschem* **79**, 781–785 (2014).

65. Myrgorodska, I., Meinert, C., Martins, Z., le Sergeant d'Hendecourt, L. & Meierhenrich, U. J. Quantitative enantioseparation of amino acids by comprehensive two-dimensional gas chromatography applied to non-terrestrial samples. *J. Chromatogr. A* **1433**, 131–136 (2016).

66. d'Hendecourt, L. & Dartois, E. Interstellar matrices: the chemical composition and evolution of interstellar ices as observed by ISO . *Spectrochim. Acta. A* **57**, 669–684 (2001).

FIGURES AND TABLES

Supplementary Information

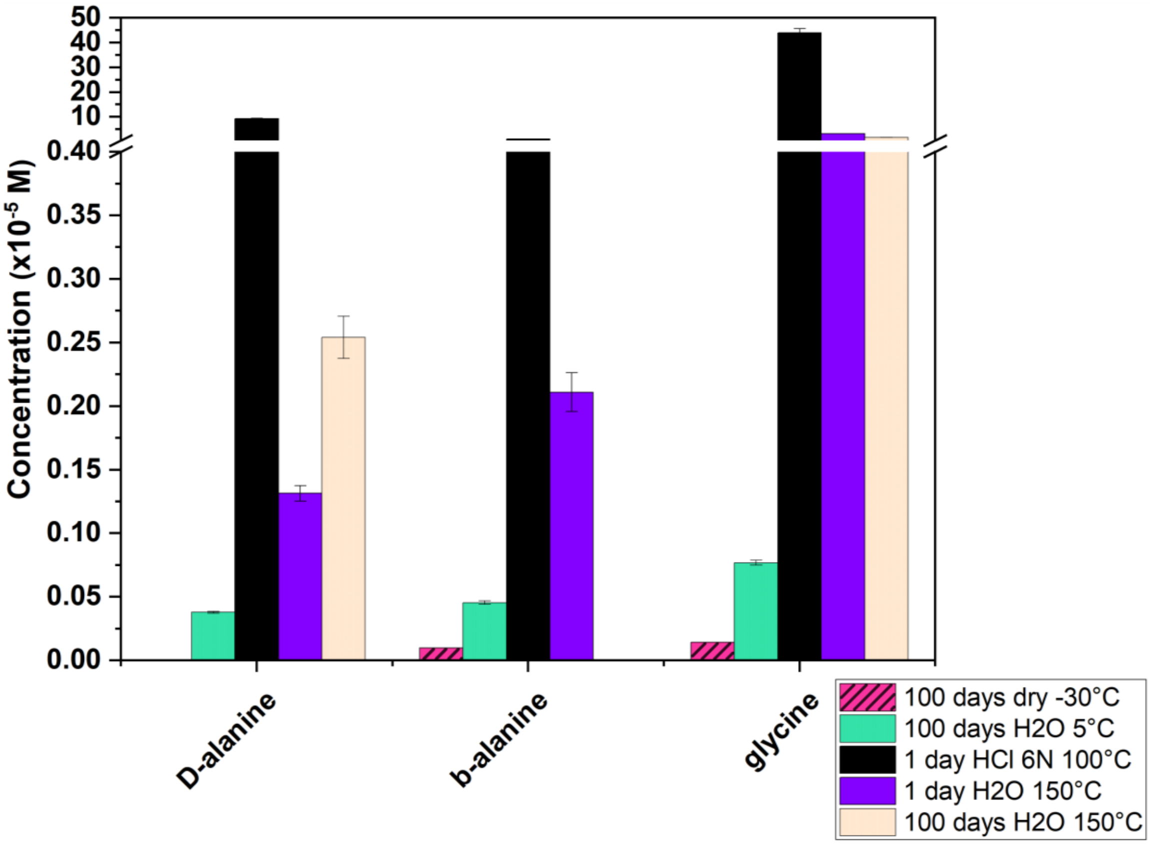

Figure S1 – Concentration of D-alanine, β-alanine and glycine after 1 day in water at 150 °C or in HCl 6N at 110 °C compared to data displayed in Figure 1 for the initial pre-accretional analog (stored at -30°C in dry condition), and after 100 days in water at 5 °C or 150 °C. β-alanine and glycine in the pre-accretional analog (dry at -30 °C) are dashed because observed but below the quantification limit.

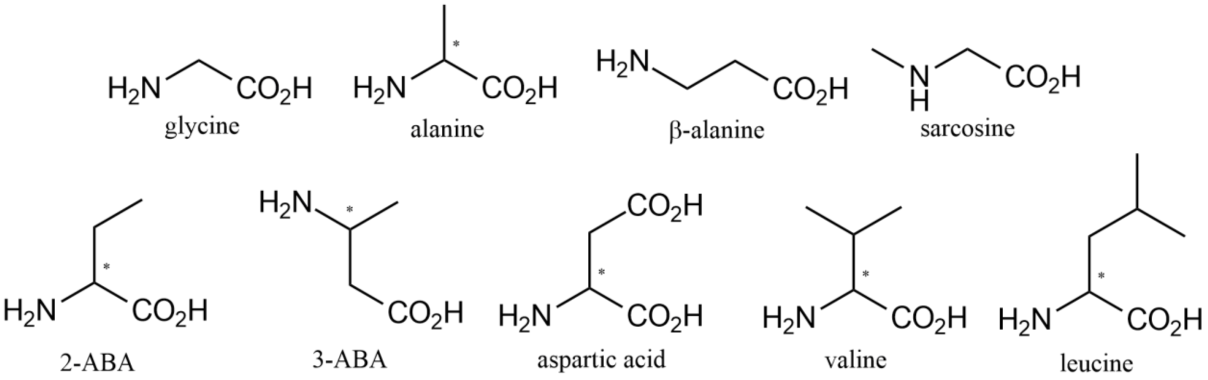

Figure S2 – Amino acid structures observed in the different experiments to estimate the impact of aqueous alteration on the content and evolution of amino acids in a pre-accretional analogue.

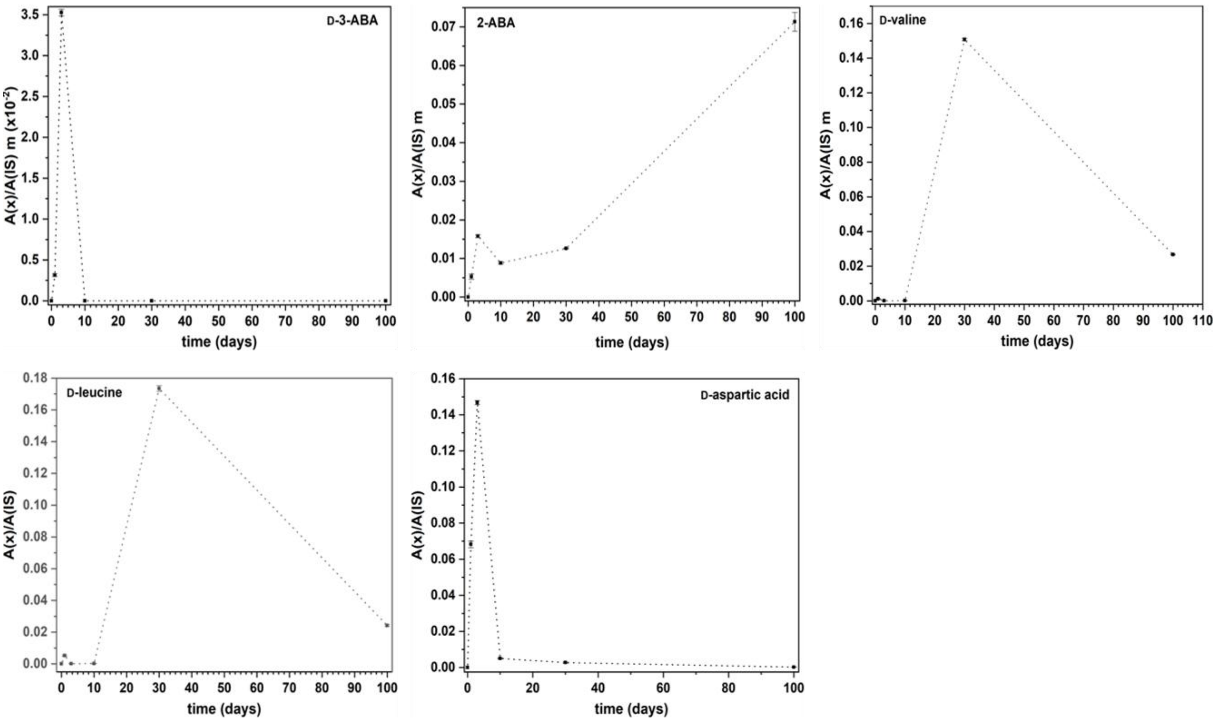

Figure S3 – Monitoring of relative intensities of integrated areas of sample (amino acids, A(x)) against internal standard (A(IS)) for several amino acids in a pre-accretional analogue incubated at 150 °C in water. The curves are only intended to serve as a visual guide.

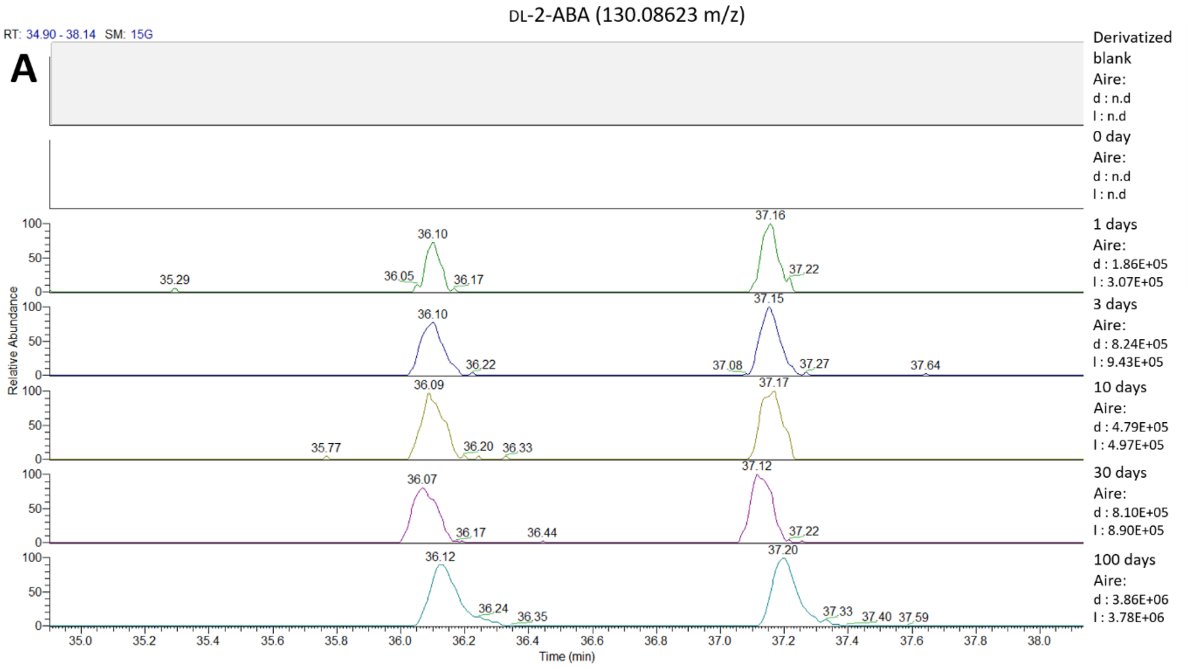
DL-2-ABA (130.08623 m/z)
RT: 34.90 - 38.14 SM: 15G
A
Derivatized blank
Aire:
d : n.d
l : n.d
0 day
Aire:
d : n.d
l : n.d
1 days
Aire:
d : 1.86E+05
l : 3.07E+05
3 days
Aire:
d : 8.24E+05
l : 9.43E+05
10 days
Aire:
d : 4.79E+05
l : 4.97E+05
30 days
Aire:
d : 8.10E+05
l : 8.90E+05
100 days
Aire:
d : 3.86E+06
l : 3.78E+06
35.29
36.05
36.10
36.17
37.16
37.22
36.10
36.22
37.08
37.15
37.27
37.64
35.77
36.09
36.20
36.33
37.17
36.07
36.17
36.44
37.12
37.22
36.12
36.24
36.35
37.20
37.33
37.40
37.59
Relative Abundance
100
50
0
35.0
35.2
35.4
35.6
35.8
36.0
36.2
36.4
36.6
36.8
37.0
37.2
37.4
37.6
37.8
38.0
Time (min)

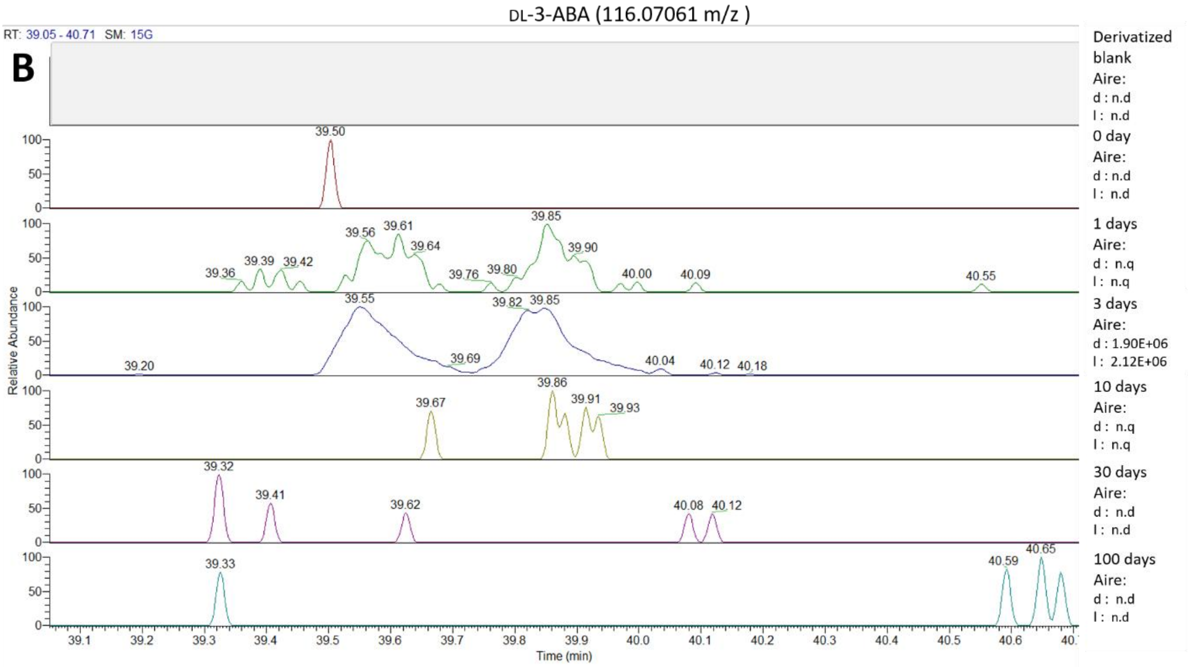
DL-3-ABA (116.07061 m/z)
RT: 39.05 - 40.71 SM: 15G
B
Derivatized blank
Aire:
d : n.d
l : n.d
0 day
Aire:
d : n.d
l : n.d
1 days
Aire:
d : n.q
l : n.q
3 days
Aire:
d : 1.90E+06
l : 2.12E+06
10 days
Aire:
d : n.q
l : n.q
30 days
Aire:
d : n.d
l : n.d
100 days
Aire:
d : n.d
l : n.d
39.50
39.36
39.39
39.42
39.56
39.61
39.64
39.76
39.80
39.85
39.90
40.00
40.09
40.55
39.20
39.55
39.69
39.82
39.85
40.04
40.12
40.18
39.67
39.86
39.91
39.93
39.32
39.41
39.62
40.08
40.12
39.33
40.59
40.65
Relative Abundance
100
50
0
39.1
39.2
39.3
39.4
39.5
39.6
39.7
39.8
39.9
40.0
40.1
40.2
40.3
40.4
40.5
40.6
40.
Time (min)

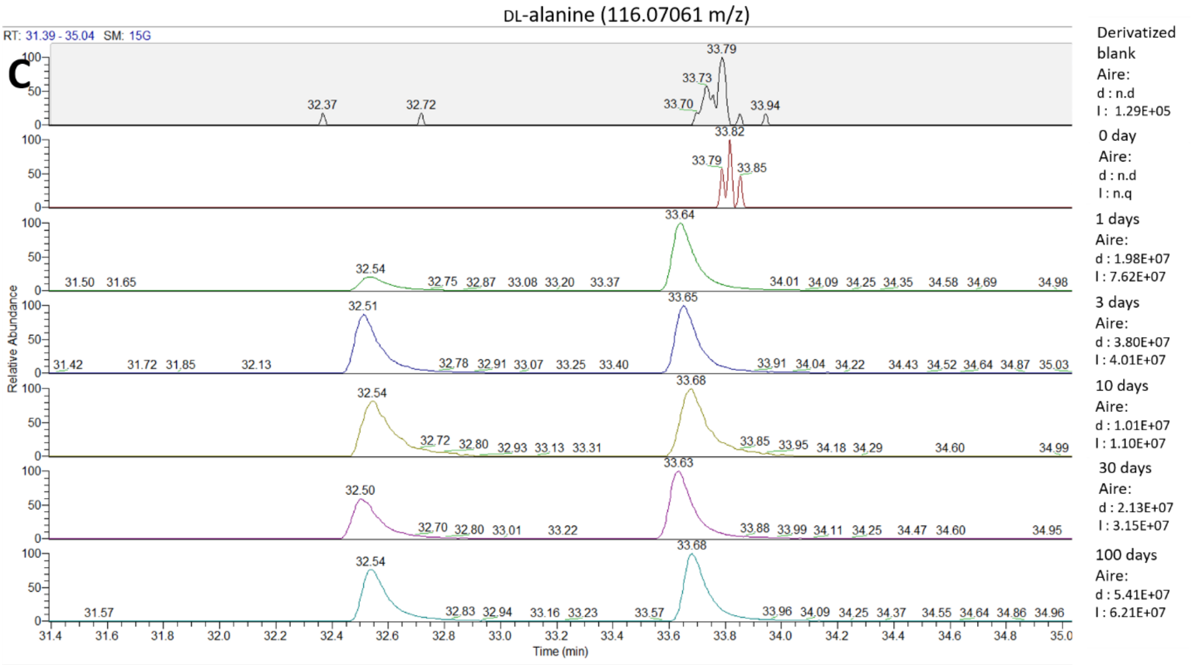
DL-alanine (116.07061 m/z)
RT: 31.39 - 35.04 SM: 15G
C
Relative Abundance
Time (min)
33.79
33.82
33.64
32.51
33.65
32.54
33.68
32.50
33.63
32.54
33.68
Derivatized blank
Aire:
d : n.d
l : 1.29E+05
0 day
Aire:
d : n.d
l : n.q
1 days
Aire:
d : 1.98E+07
l : 7.62E+07
3 days
Aire:
d : 3.80E+07
l : 4.01E+07
10 days
Aire:
d : 1.01E+07
l : 1.10E+07
30 days
Aire:
d : 2.13E+07
l : 3.15E+07
100 days
Aire:
d : 5.41E+07
l : 6.21E+07

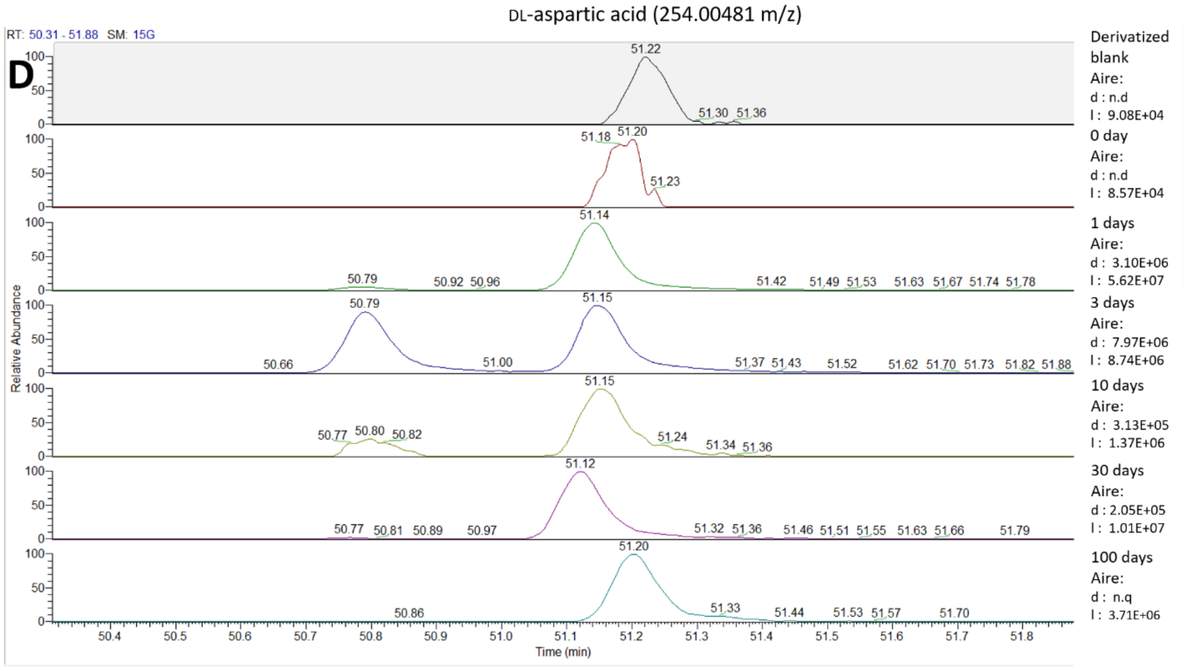
DL-aspartic acid (254.00481 m/z)
RT: 50.31 - 51.88 SM: 15G
D
Relative Abundance
Time (min)
51.22
51.20
51.14
50.79
51.15
51.15
51.12
51.20
Derivatized blank
Aire:
d : n.d
l : 9.08E+04
0 day
Aire:
d : n.d
l : 8.57E+04
1 days
Aire:
d : 3.10E+06
l : 5.62E+07
3 days
Aire:
d : 7.97E+06
l : 8.74E+06
10 days
Aire:
d : 3.13E+05
l : 1.37E+06
30 days
Aire:
d : 2.05E+05
l : 1.01E+07
100 days
Aire:
d : n.q
l : 3.71E+06

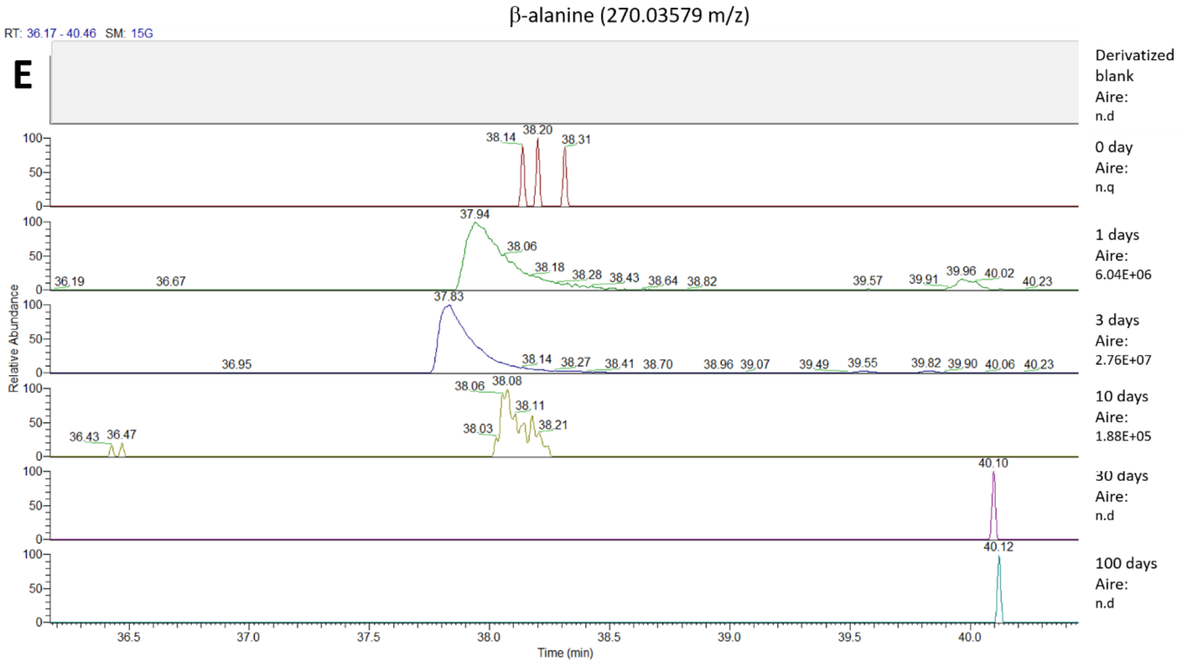
β-alanine (270.03579 m/z)
RT: 36.17 - 40.46 SM: 15G
E
Derivatized blank Aire: n.d
0 day Aire: n.q
1 days Aire: 6.04E+06
3 days Aire: 2.76E+07
10 days Aire: 1.88E+05
30 days Aire: n.d
100 days Aire: n.d
38.14
38.20
38.31
37.94
38.06
38.18
38.28
38.43
38.64
38.82
36.19
36.67
39.57
39.91
39.96
40.02
40.23
37.83
36.95
38.14
38.27
38.41
38.70
38.96
39.07
39.49
39.55
39.82
39.90
40.06
40.23
38.06
38.08
38.11
38.03
38.21
36.43
36.47
40.10
40.12
Relative Abundance
0
50
100
36.5
37.0
37.5
38.0
38.5
39.0
39.5
40.0
Time (min)

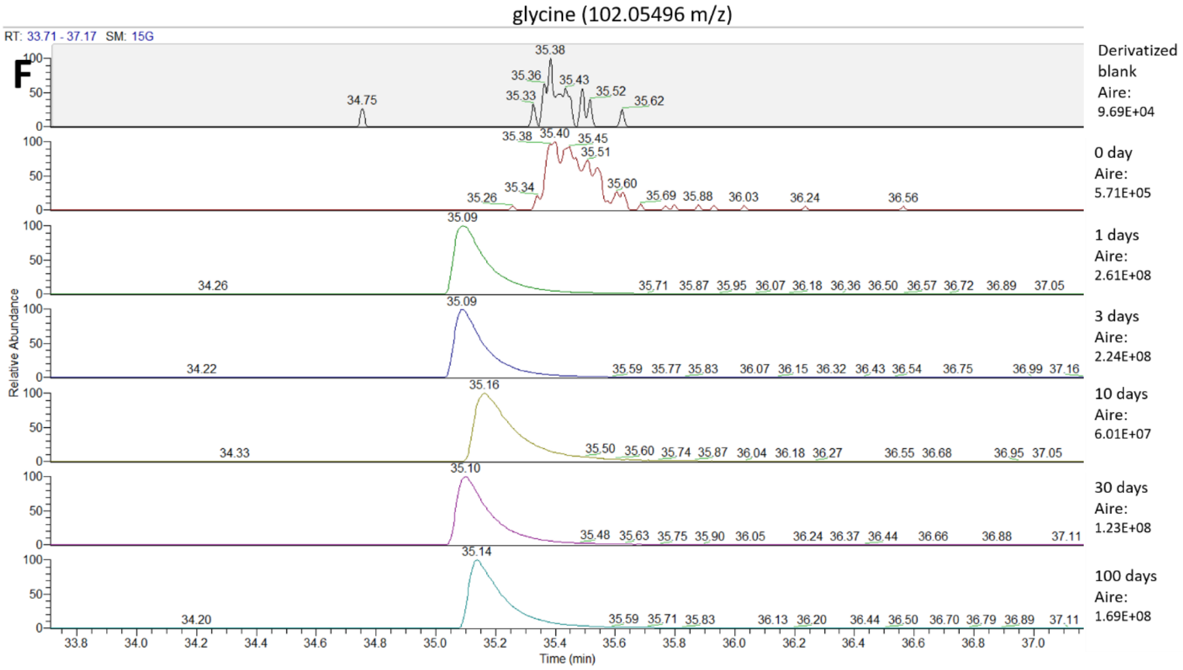
glycine (102.05496 m/z)
RT: 33.71 - 37.17 SM: 15G
F
Derivatized blank Aire: 9.69E+04
0 day Aire: 5.71E+05
1 days Aire: 2.61E+08
3 days Aire: 2.24E+08
10 days Aire: 6.01E+07
30 days Aire: 1.23E+08
100 days Aire: 1.69E+08
34.75
35.33
35.36
35.38
35.43
35.52
35.62
35.26
35.34
35.38
35.40
35.45
35.51
35.60
35.69
35.88
36.03
36.24
36.56
35.09
34.26
35.71
35.87
35.95
36.07
36.18
36.36
36.50
36.57
36.72
36.89
37.05
35.09
34.22
35.59
35.77
35.83
36.07
36.15
36.32
36.43
36.54
36.75
36.99
37.16
35.16
34.33
35.50
35.60
35.74
35.87
36.04
36.18
36.27
36.55
36.68
36.95
37.05
35.10
35.48
35.63
35.75
35.90
36.05
36.24
36.37
36.44
36.66
36.88
37.11
35.14
34.20
35.59
35.71
35.83
36.13
36.20
36.44
36.50
36.70
36.79
36.89
37.11
Relative Abundance
0
50
100
33.8
34.0
34.2
34.4
34.6
34.8
35.0
35.2
35.4
35.6
35.8
36.0
36.2
36.4
36.6
36.8
37.0
Time (min)

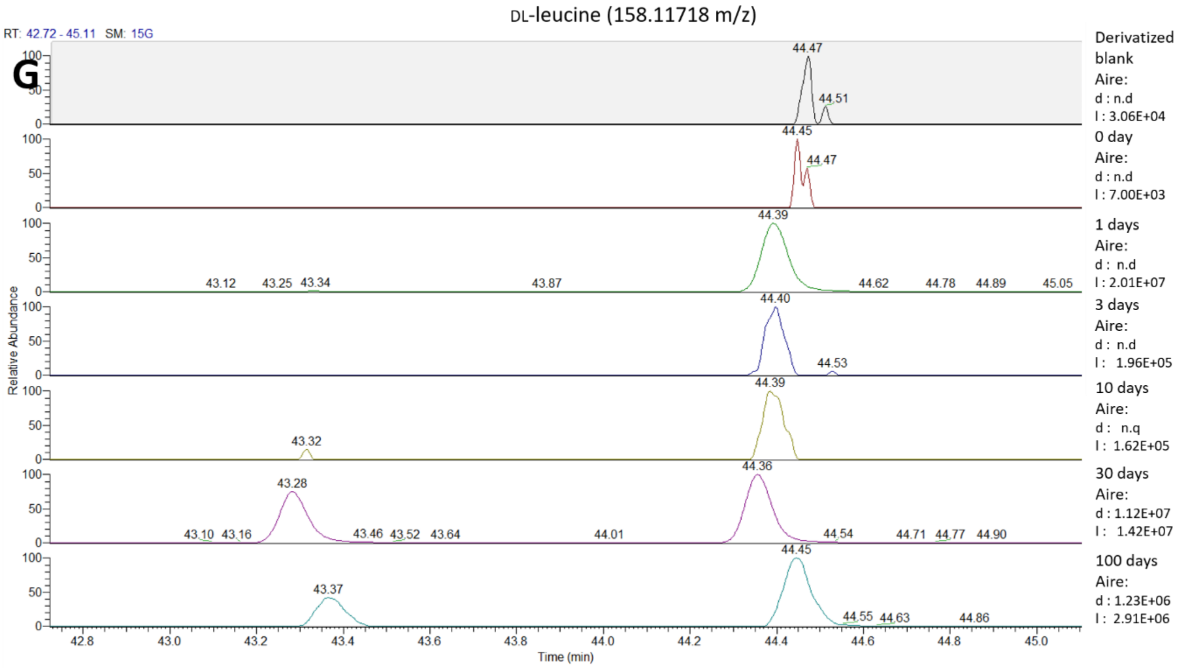
DL-leucine (158.11718 m/z)
RT: 42.72 - 45.11 SM: 15G
G
Relative Abundance
Time (min)
42.8
43.0
43.2
43.4
43.6
43.8
44.0
44.2
44.4
44.6
44.8
45.0
44.47
44.51
44.45
44.47
44.39
43.12
43.25
43.34
43.87
44.62
44.78
44.89
45.05
44.40
44.53
44.39
43.32
44.36
43.28
43.10
43.16
43.46
43.52
43.64
44.01
44.54
44.71
44.77
44.90
44.45
43.37
44.55
44.63
44.86
Derivatized blank
Aire:
d : n.d
I : 3.06E+04
0 day
Aire:
d : n.d
I : 7.00E+03
1 days
Aire:
d : n.d
I : 2.01E+07
3 days
Aire:
d : n.d
I : 1.96E+05
10 days
Aire:
d : n.q
I : 1.62E+05
30 days
Aire:
d : 1.12E+07
I : 1.42E+07
100 days
Aire:
d : 1.23E+06
I : 2.91E+06

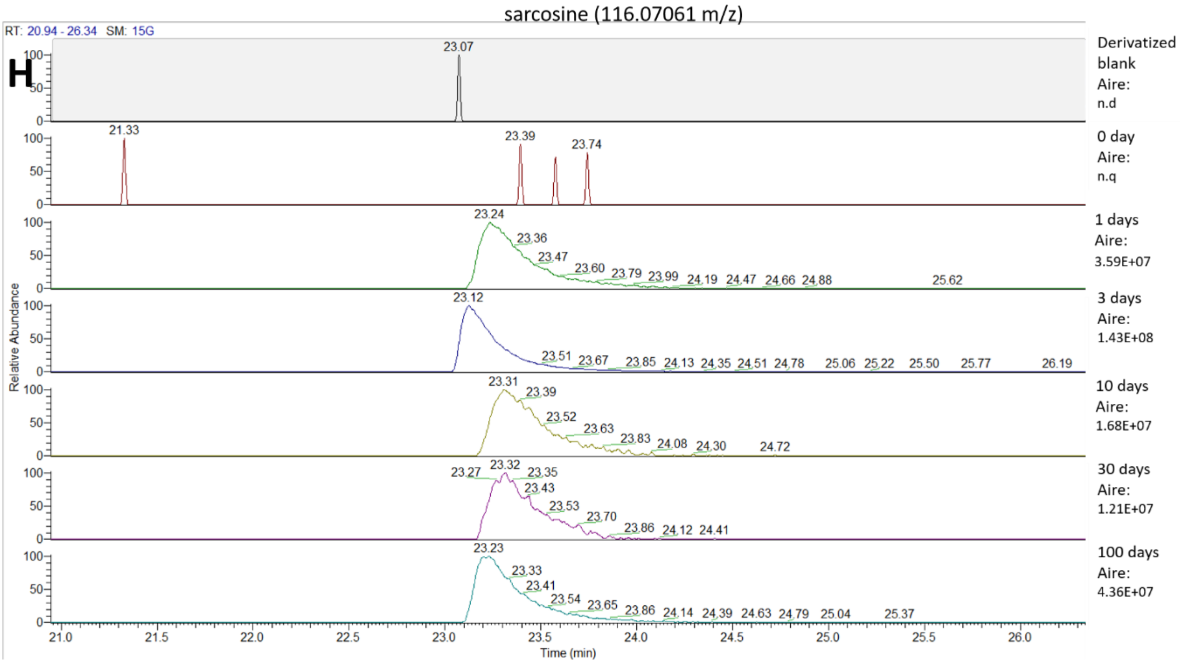
sarcosine (116.07061 m/z)
RT: 20.94 - 26.34 SM: 15G
H
Relative Abundance
Time (min)
21.0
21.5
22.0
22.5
23.0
23.5
24.0
24.5
25.0
25.5
26.0
23.07
21.33
23.39
23.74
23.24
23.36
23.47
23.60
23.79
23.99
24.19
24.47
24.66
24.88
25.62
23.12
23.51
23.67
23.85
24.13
24.35
24.51
24.78
25.06
25.22
25.50
25.77
26.19
23.31
23.39
23.52
23.63
23.83
24.08
24.30
24.72
23.27
23.32
23.35
23.43
23.53
23.70
23.86
24.12
24.41
23.23
23.33
23.41
23.54
23.65
23.86
24.14
24.39
24.63
24.79
25.04
25.37
Derivatized blank
Aire:
n.d
0 day
Aire:
n.q
1 days
Aire:
3.59E+07
3 days
Aire:
1.43E+08
10 days
Aire:
1.68E+07
30 days
Aire:
1.21E+07
100 days
Aire:
4.36E+07

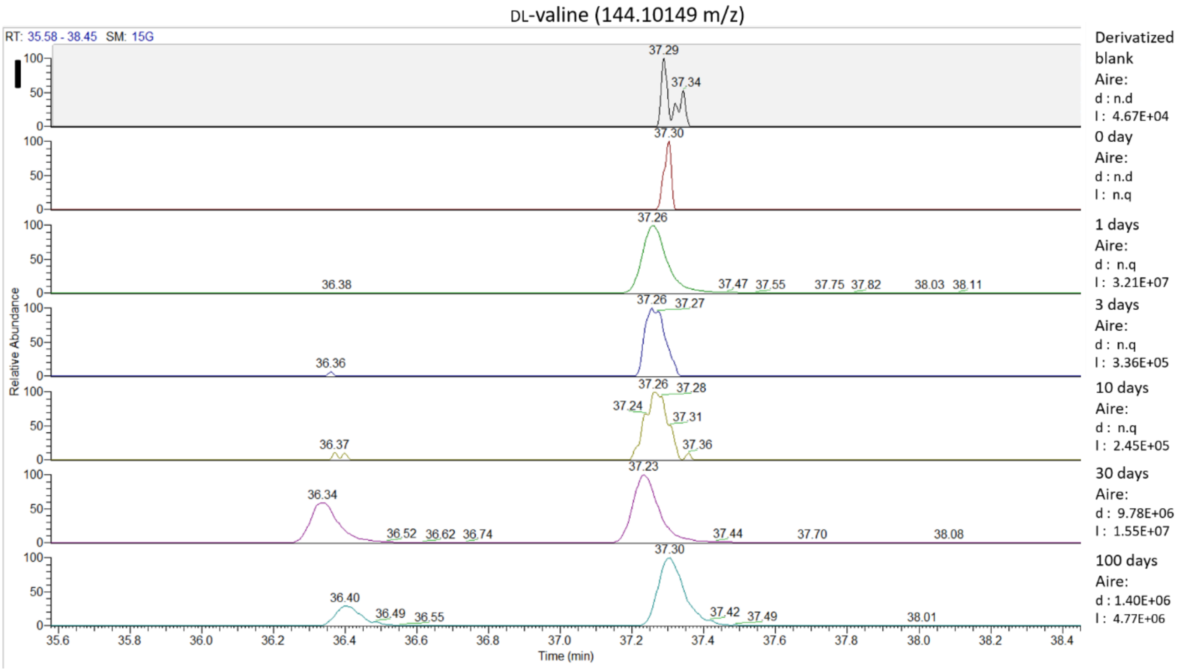

Figure S4 - Chromatograms of the different amino acids monitored during the aqueous alteration of pre-accretional organic analog at 150 °C under 6 bars for different duration (0 day corresponds to the initial pre-accretional analog, 1, 3, 10, 30 and 100 days). All data are mass extraction of the characteristic mass of a given amino acids on full scan. Are also reported the derivatized blank with the extracted mass corresponding to the one of the amino acid monitored. n.d: not detected, n.q: detected but under the limit of quantification. (A) DL-2-ABA, (B) DL-3-ABA, (C) DL-alanine, (D) DL-aspartic acid, (E) β-alanine, (F) glycine, (G) DL-leucine, (H) sarcosine, and (I) DL-valine.

Theoretical m/z	Exp. m/z	Neutral formula	Amadori rearrangement product (ARP)	100 days dry -30°C	100 day H2O 5°C	1 day H2O 150°C	3 day H2O 150°C	10 day H2O 150°C	30 day H2O 150°C	100 day H2O 150°C
130.05096	130.05097	C5H9NO3	alanine/b-alanine/sarcosine-glycolaldehyde-ARP	2504102	0	4210929	5894227	0	0	0
144.06661	144.06662	C6H11NO3	2-ABA/d-3-ABA-glycolaldehyde-ARP	3396545	2646139	3261884	4609152	3116913	3452400	2945875
174.0407	174.04079	C6H9NO5	aspartic acid-glycolaldehyde-ARP	32279092	26941404	11379647	19023838	4660976	4160652	4279944
158.08226	158.08225	C7H13NO3	valine-glycolaldehyde-ARP	2797453	1447346	1697093	3666564	4045417	4751750	5021589
172.09791	172.09793	C8H15NO3	leucine-glycolaldehyde-ARP	2464198	8994665	2327955	3279901	3999619	5680488	6898776
146.04588	146.04588	C5H9NO4	glycine-triose-ARP	25319092	44844088	14673530	16048065	2969381	7242917	2404041
160.06153	160.06153	C6H11NO4	alanine/b-alanine/sarcosine-triose-ARP	25382206	37197804	16770200	25017896	4485142	6724031	7736155
174.07718	174.07685	C7H13NO4	2-ABA/d-3-ABA-triose-ARP	4145765	6250220	3895090	6620017	2780961	8048164	7625521
204.05136	204.05135	C7H11NO6	aspartic acid-triose-ARP	84323056	73907280	35776120	62137104	12129185	22705778	15843103
188.09283	188.09283	C8H15NO4	valine-triose-ARP	11484519	21144504	13934038	25349746	17008968	26520988	15194823
202.10848	202.10848	C9H17NO4	leucine-triose-ARP	4211419	6438216	14764764	11566977	16264553	30503730	10765309
176.05644	176.05645	C6H11NO5	glycine-tetrose-ARP	84315360	86590232	17822524	21160816	3067418	3402872	1856640
190.07209	190.07210	C7H13NO5	alanine/b-alanine/sarcosine-tetrose-ARP	121093376	87451672	29142686	40090436	10930415	11505112	9230080
204.08774	204.08775	C8H15NO5	2-ABA/d-3-ABA-tetrose-ARP	84142872	55192704	31110832	72696648	24399826	22824616	20070228
234.06192	234.06192	C8H13NO7	aspartic acid-tetrose-ARP	73953000	79589704	20054210	23658860	6643664	9128619	6440824
218.10339	218.10339	C9H17NO5	valine-tetrose-ARP	29660786	198238048	20410032	33061466	19158206	16651592	11732101
232.11904	232.11903	C10H19NO5	leucine-tetrose-ARP	12757804	22031454	13796020	12930018	11783099	8200392	6276579

206.06701	206.06701	C7H13NO6	glycine-pentose-ARP	164205824	202090336	25909804	33922740	9358810	5615057	3679322
220.08266	220.08265	C8H15NO6	alanine/b-alanine/sarcosine-pentose-ARP	278809824	210757344	57972504	78336640	25412460	48362912	25371796
234.09831	234.09831	C9H17NO6	2-ABA/d-3-ABA-pentose-ARP	124923640	83759456	33237214	45490564	17321954	19191494	16100242
264.07249	264.07251	C9H15NO8	aspartic acid-pentose-ARP	59848004	65914880	10756142	15339759	2558129	3997815	2379849
248.11396	248.11394	C10H19NO6	valine-pentose-ARP	48825248	29257260	17254268	20095680	9543400	12939840	10325266
262.12961	262.12957	C11H21NO6	leucine-pentose-ARP	26321682	9651431	14873353	10743133	6626378	10743073	9498359
236.07757	236.07757	C8H15NO7	glycine-hexose-ARP	196473472	185832976	17743568	21104354	7854022	14654591	8492283
250.09322	250.09321	C9H17NO7	alanine/b-alanine/sarcosine-hexose-ARP	219514352	167719312	44102784	37062336	12943750	57663092	27158798
264.10887	264.10887	C10H19NO7	2-ABA/d-3-ABA-hexose-ARP	155620688	88672272	23005254	31547648	10418876	19150982	15342169
294.08305	294.08299	C10H17NO9	aspartic acid-hexose-ARP	34784644	34406720	0	0	2069278	0	0
278.12452	278.12453	C11H21NO7	valine-hexose-ARP	44238992	26914982	11805090	12690546	5969606	12416931	9540219
292.14017	292.14016	C12H23NO7	leucine-hexose-ARP	24265132	13956379	14375043	8201023	3550577	17184396	6656929

Table S1 - All possible Amadori rearrangement products (ARP) as obtained in reaction of the measured amino acids with glycolaldehyde and possible reducing sugars, including triose, tetrose, pentose, and hexose. Corresponding ARP with its neutral formula, theoretical and experimental mass of the deprotonated ions, as well as the intensity of these ions in the original material and the hydrothermal kinetic at 150°C during the 100 days.

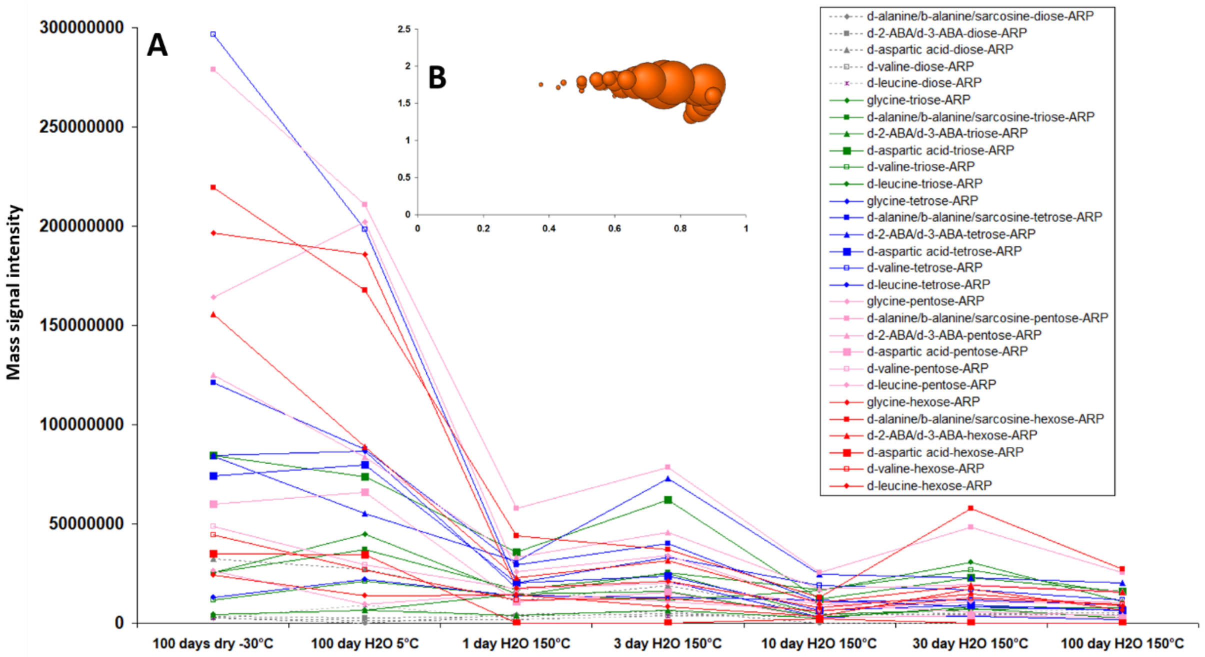

Figure S5 - (A) Time evolution of the various ARPs during hydrothermal process; (B) position in the van Krevelen diagram of the considered ARPs.

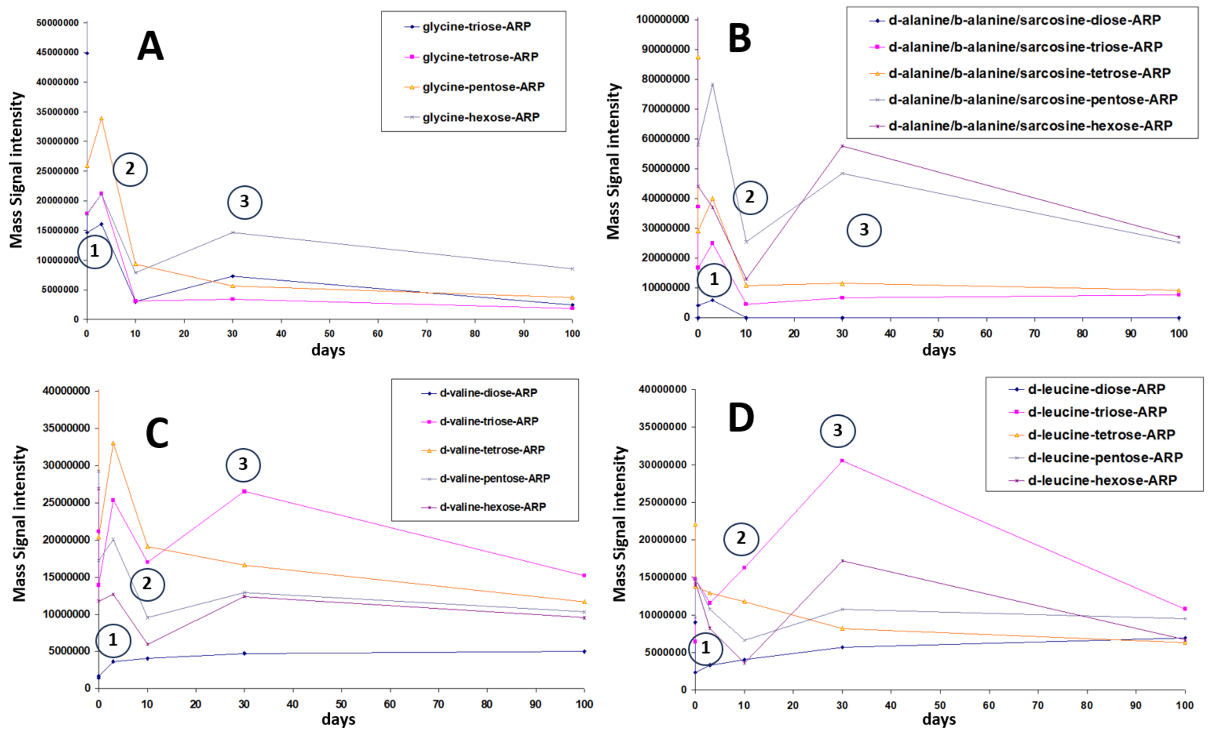

Figure S6 – (A)-(D) Time evolution of the individual ARPs (to be compared to the evolution of the individual amino acids in Figure 2) during the hydrothermal process